Colombi et al., http://www.jcb.org/cgi/content/full/jcb.201305115/DC1

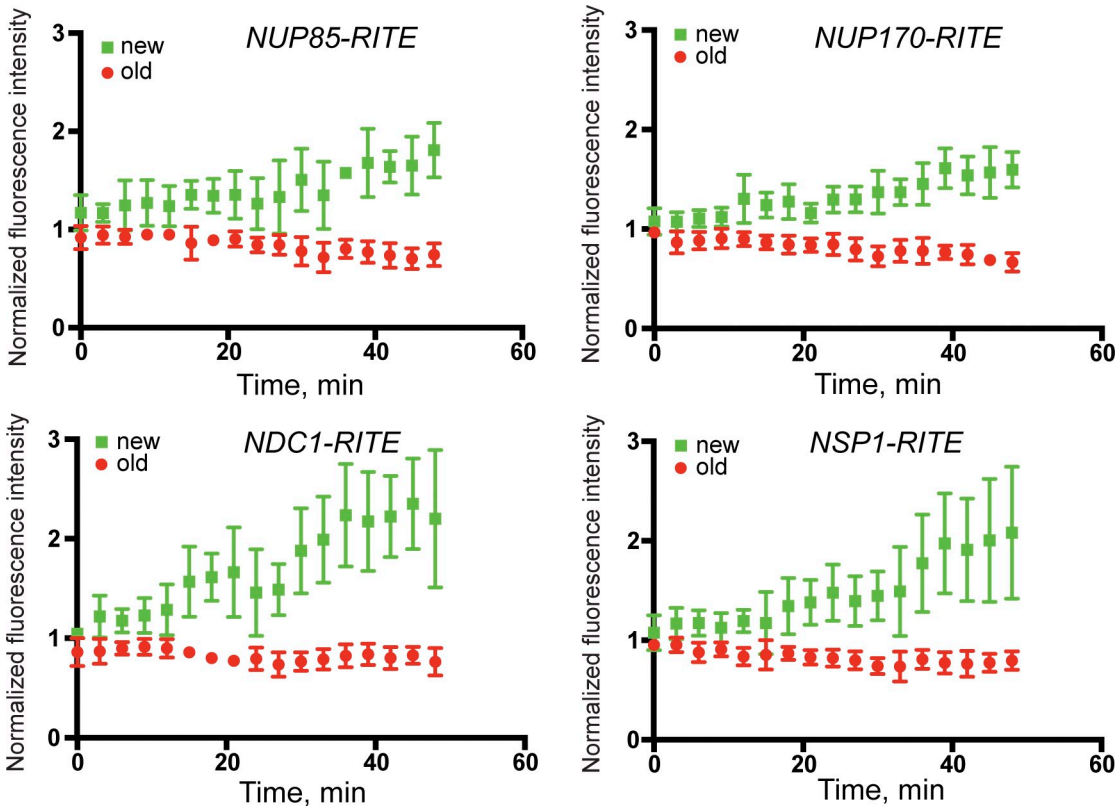

Figure S1. **Nup-mCherry levels do not increase after RITE.** Yeast strains expressing the indicated *NUP-RITE* alleles (PCCPL520, PCCPL522, PCCPL526, and WZCPL2) were grown in the presence of estradiol. Unbudded/small budded cells were imaged every 3 min. The total fluorescence of "new" Nup-GFP and "old" Nup-mCherry was measured at each time point, and these numbers were normalized to the minimum value (GFP) or the maximum value (mCherry). The normalized values are plotted against time (min). Error bars are the standard deviation from the mean. $n = 6$.

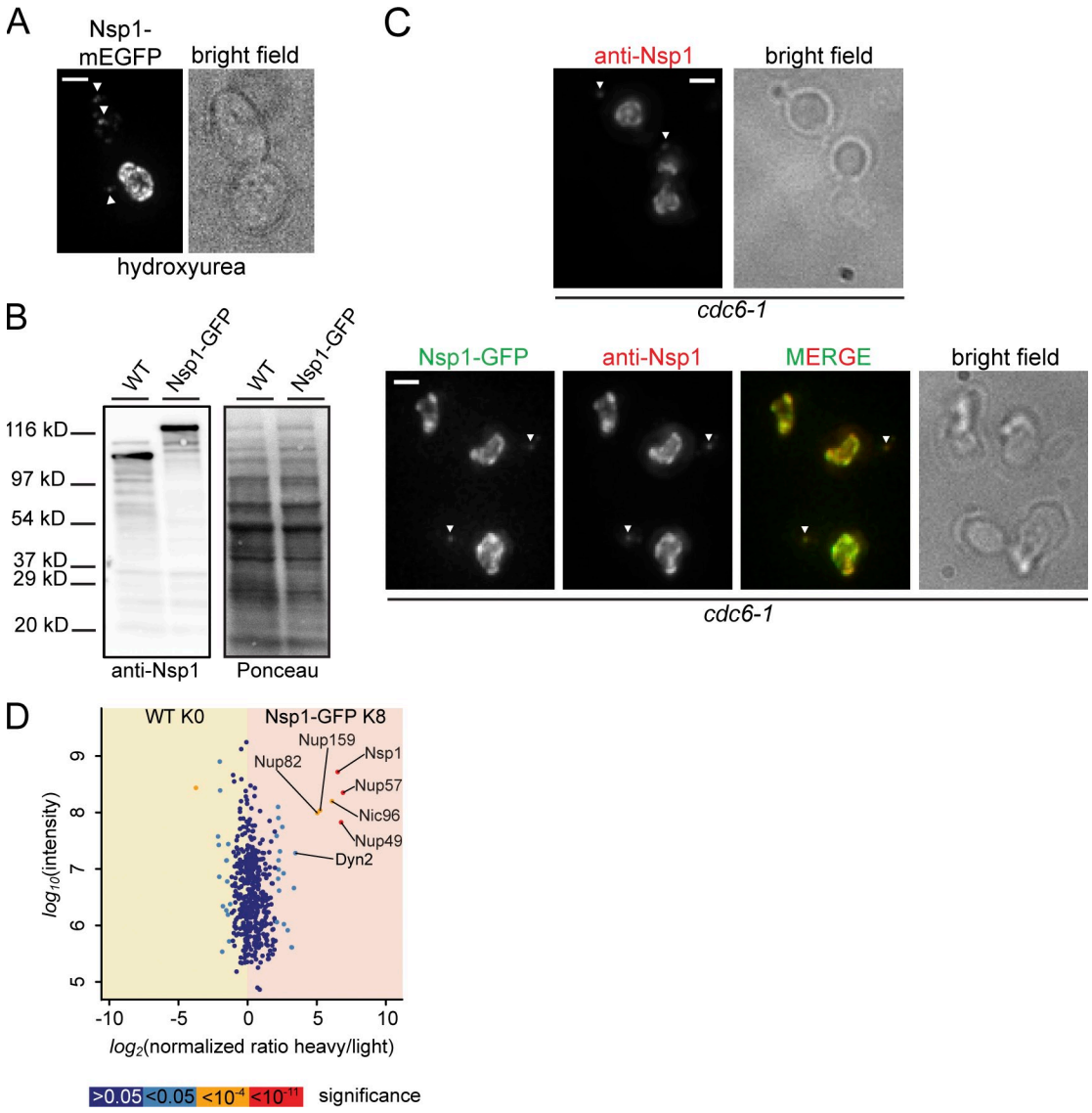

Figure S2. **Nsp1-GFP is functional.** (A) A fluorescence micrograph (and bright field) of a z series of deconvolved images of cells expressing Nsp1-mEGFP (PCCPL468) after arrest in S phase with hydroxyurea. To visualize cytoplasmic foci (arrowheads), maximum-intensity projections are shown and contrast was digitally enhanced to saturate 0.4% of pixels. Bar, 2 µm. (B) Western blots of total protein (stained with Ponceau; right) from whole cell extracts derived from wild-type (WT/W303) and Nsp1-GFP–containing strains (CPL1234). Detection of Nsp1 (left) was performed using anti-Nsp1 antibodies followed by HRP-conjugated secondary antibodies and ECL. (C) Immunofluorescence of *cdc6-1* (YB0044; top) or *cdc6-1* expressing Nsp1-GFP (PCCPL393; bottom). Anti-Nsp1 antibodies followed by Alexa Fluor 594–conjugated secondary antibodies were used to detect Nsp1 or Nsp1-GFP. Images are a maximum-intensity projection of a z series of deconvolved images. Arrowheads point to bud-localized Nsp1 foci. Bars, 2 µm. (D) Plot showing the enrichment of heavy-labeled (K8) compared to light-labeled (K0) peptides from an anti-GFP affinity purification of cell extracts derived from WT (PCCPL329) or Nsp1-GFP (PCCPL322)–containing strains. Averaged peptide intensities are plotted against heavy (K8)/light (K0) SILAC ratios. Significant outliers are colored as indicated by the legend.

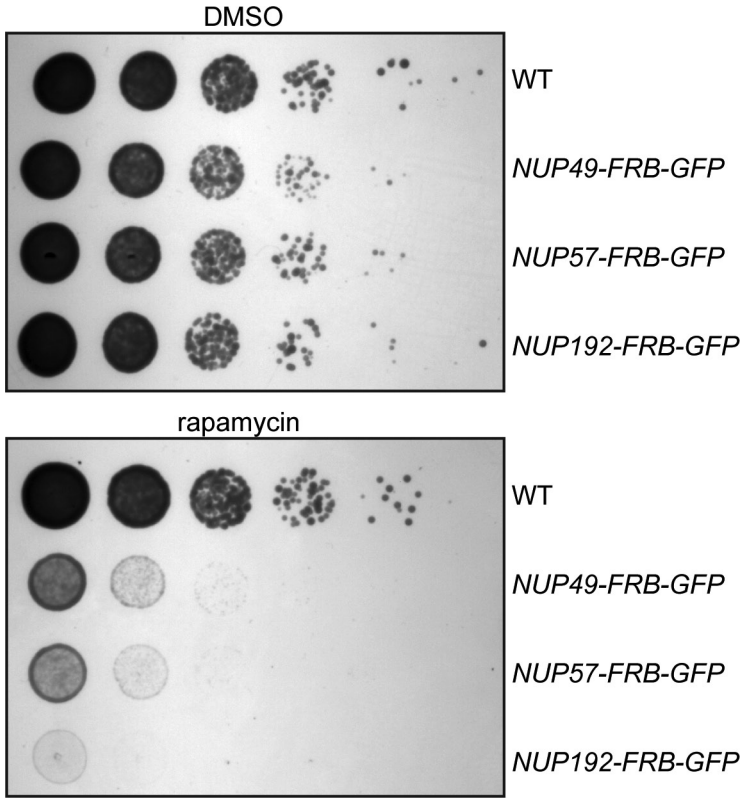

Figure S3. **Trapping of Nup-FRB-GFP fusion proteins leads to loss of cell growth.** Yeast strains expressing the indicated Nup-FRB-GFP fusions (CPL1238, CPL1239, and PCCPL304) were plated alongside WT cells (HHY110) in 10-fold serial dilutions on YPD containing rapamycin or carrier alone (DMSO). Plates were imaged after 48 h at 30°C.

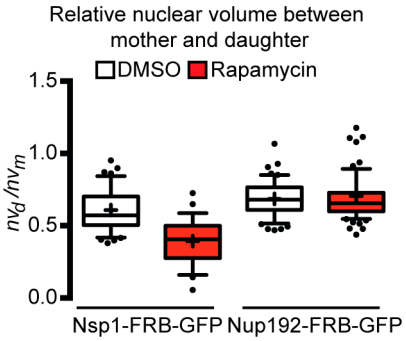

Figure S4. **Reduction of nuclear size after trapping of Nsp1-FRB-GFP$_{CYT}$.** A box plot comparing daughter/mother nuclear volume (nv_d/nv_m) ratios of Nsp1-FRB-GFP or Nup192-FRB-GFP cells after anaphase completion in DMSO- or rapamycin-treated conditions. $36 \leq n \leq 96$. Box and whisker percentiles as in Fig. 3.

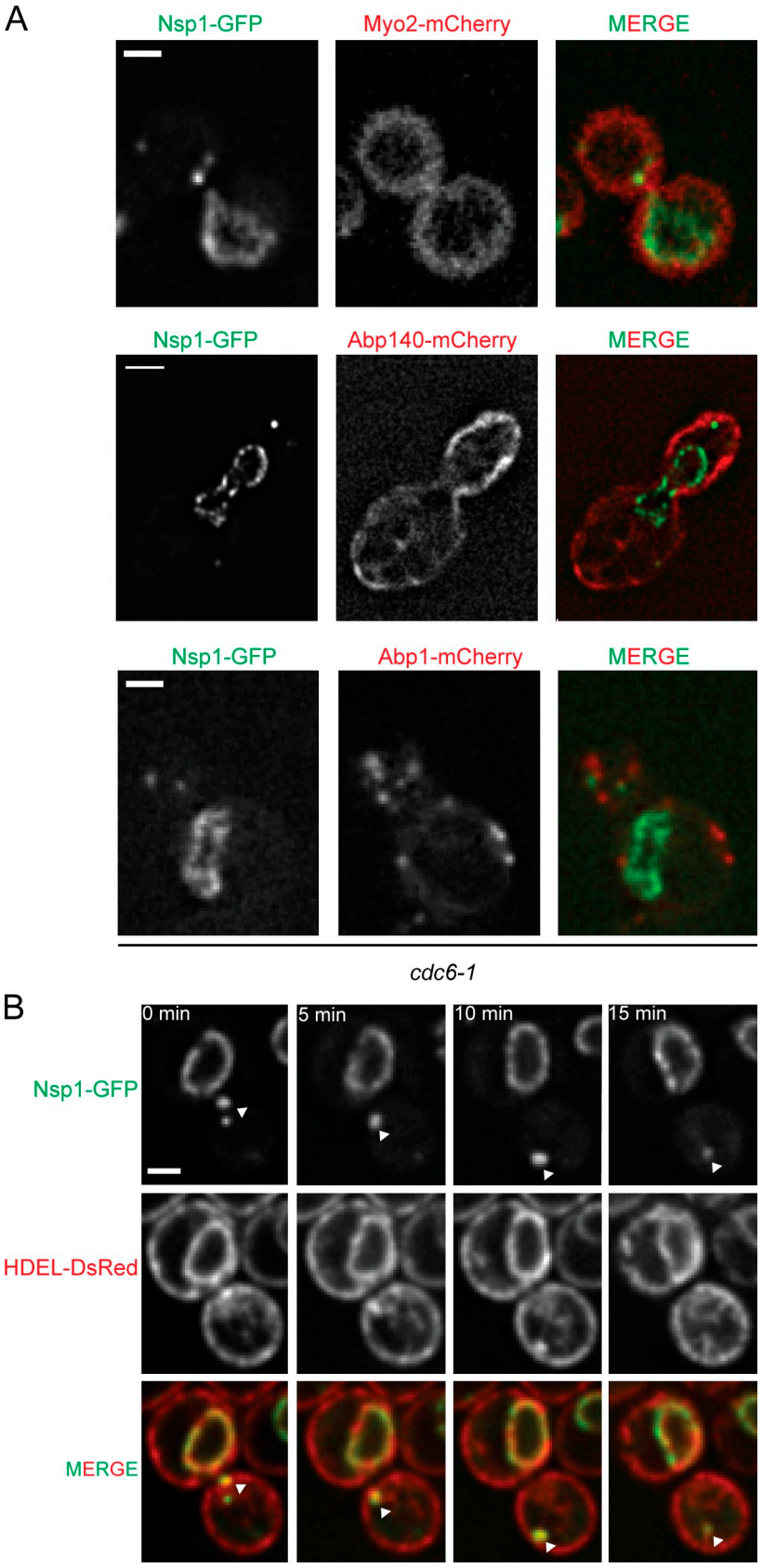

Figure S5. **Nsp1-GFP does not colocalize with Myo2 and actin but associates with ER.** (A) Deconvolved fluorescence micrographs of a z section of *cdc6-1* cells expressing Nsp1-GFP and either Myo2-mCherry (PCCPL542), Abp140-mCherry (PCCPL543), or Abp1-mCherry (PCCPL534), with a merged image. Bars, 2 µm. (B) Time-lapse series (Δt = 5 min) of PCCPL533 expressing Nsp1-GFP and HDEL-mRFP. At each time point, the one z plane of a deconvolved z series where the Nsp1-GFP overlaps with the bolus of ER traveling from the mother NE to the daughter cortex (arrowheads) is shown in green and red channels along with the merge. Bar, 2 µm.

Table S1. **Yeast strains**

Name	Genotype	Source
W303	*ade2-1 can1-100 his3-11,15 leu2-3,112 trp1-1 ura3-1*	Euroscarf
ABY530	*MAT alpha myo2-20::HIS3 his3-D200 ura3-52 leu2-3,112 lys2-801 ade2-101 Gal+*	Gift from A. Bretscher (Schott et al., 1999)
ABY534	*MAT alpha myo2-14::HIS3 his3-D200 ura3-52 leu2-3,112 lys2-801 ade2-101 Gal+*	Gift from A. Bretscher (Schott et al., 1999)
HHY110	W303, *MAT alpha tor1-1 fpr1Δ::natMX6 PMA1-2×FKBP12::TRP1*	Euroscarf (Haruki et al., 2008)
YB0044	*MAT a ade2 leu2 ura3 trp1 his3 can1 cdc6-1*	Gift from B. Stillman (Liang et al., 1995)
BWCPL42	W303, *NUP85-GFP::kanMX6*	PCR-based integration using pFA6a-GFP-kanMX6
BWCPL433	W303, *POM34-GFP::kanMX6*	PCR-based integration using pFA6a-GFP-kanMX6
BWCPL437	W303, *NUP170-GFP::kanMX6*	PCR-based integration using pFA6a-GFP-kanMX6
CPL1229	HHY110, *NSP1-FRB-GFP::His3MX6 NUP170-mCherry::kanMX6*	PCR-based integration using pFA6a-mCherry-kanMX6 and pFA6a-FRB-GFP-His3MX6
CPL1231	HHY110, *NSP1-FRB::His3MX6 NUP133-2xDendra::URA*	PCR-based integration using pFA6a-FRB-His3MX6 and integration of pKW2329 cut with HindIII
CPL1234	W303, *NSP1-GFP::His3MX6*	PCR-based integration using pFA6a-GFP-His3MX6
CPL1238	HHY110, *NUP49-FRB-GFP::His3MX6*	PCR-based integration using pFA6a-FRB-GFP-His3MX6
CPL1239	HHY110, *NUP57-FRB-GFP::His3MX6*	PCR-based integration using pFA6a-FRB-GFP-His3MX6
CVCPL01	W303, *NUP57-GFP::His3MX6*	PCR-based integration using pFA6a-FRB-GFP-His3MX6
PCCPL65	W303, *myo4Δ::hphMX6*	PCR-based integration using pFA6a-hphMX6
PCCPL168	W303, *NIC96-GFP::His3MX6*	PCR-based integration using pFA6a-GFP-His3MX6
PCCPL251	HHY110, *NIC96-FRB::His3MX6*	PCR-based integration using pFA6a-FRB-His3MX6
PCCPL259	HHY110, *NSP1-FRB-GFP::His3MX6*	PCR-based integration using pFA6a-FRB-GFP-His3MX6
PCCPL260	HHY110, *NSP1-FRB::His3MX6*	PCR-based integration using pFA6a-FRB-His3MX6
PCCPL293	HHY110, *NIC96-FRB-GFP::His3MX6 Nup170-mCherry::kanMX6*	PCR-based integration using pFA6a-mCherry-kanMX6 and pFA6a-FRB-GFP-His3MX6
PCCPL302	HHY110, *NIC96-FRB-GFP::His3MX6*	PCR-based integration using pFA6a-FRB-GFP-His3MX6
PCCPL304	HHY110, *NUP192-FRB-GFP::His3MX6*	PCR-based integration using pFA6a-FRB-GFP-His3MX6
PCCPL314	W303, *lys2Δ::natMX6 bar1Δ::hphMX6*	PCR-based integration using pFA6a-hphMX6 and pFA6a-natMX6
PCCPL315	W303, *NSP1-GFP::His3MX6*	PCR-based integration using pFA6a- GFP-His3MX6
PCCPL316	ABY530, *NSP1-GFP::kanMX6*	PCR-based integration using pFA6a-GFP-kanMX6
PCCPL317	ABY534, *NSP1-GFP::kanMX6*	PCR-based integration using pFA6a-GFP-kanMX6
PCCPL322	W303, *lys2Δ::natMX6 bar1Δ::hphMX6 NSP1-GFP::His3MX6*	Progeny from cross PCCPL314 and PCCPL315
PCCPL365	W303, *NSP1-GFP::His3MX6 myo4Δ::hphMX6*	Progeny from cross of CPL1234 and PCCPL65
PCCPL392	YB0044, *NUP170-GFP::TRP1*	PCR-based integration using pFA6a-GFP-TRP1
PCCPL393	YB0044, *NSP1-GFP::TRP1*	PCR-based integration using pFA6a-GFP-TRP1
PCCPL397	*CLB2-TAP::HIS3 GAL-SWE1-myc::LEU, bar1*	DLY7808; gift from D.J. Lew (Keaton et al., 2007)
PCCPL409	PCCPL397, *NSP1-GFP::kanMX6*	PCR-based integration using pFA6a-GFP-kanMX6
PCCPL416	W303, *dyn2Δ:: hphMX6*	PCR-based integration using pFA6a-hphMX6
PCCPL423	PCCPL397, *NUP170-GFP::kanMX6*	PCR-based integration using pFA6a-GFP-kanMX6
PCCPL427	PCCPL416, *NSP1-GFP::His3MX6*	Progeny from cross CPL1234 and PCCPL416
PCCPL445	PCCPL416, *NUP85-GFP::kanMX6*	Progeny from cross BWCPL42 and PCCPL416
PCCPL468	*NSP1-mEGFP::kanMX6*	PCR-based integration using pFA6a-mEGFP-kanMX6
PCCPL487	HHY110, *NSP1-FRB-GFP::His3MX6 HMG1-mCherry::kanMX6*	PCR-based integration using pFA6a-mCherry-kanMX6 and pFA6a-FRB-GFP-His3MX6
PCCPL506	*kanMX6::pGAL1-3HA-SWE1 NSP1-loxP-HA-mCherry-HYG-loxP-GFP CRE-EBD78::HIS3*	PCR-based integration using PLPMR2, pFa6a-kanMX6-GAL1-HA and integration of pTW040 linearized with Eco47III
PCCPL510	HHY110, *NUP49-FRB-GFP::His3MX6 NUP170-mCherry::kanMX6*	PCR-based integration using pFA6a-mCherry-kanMX6 and pFA6a-FRB-GFP-His3MX6
PCCPL511	*HHY110 NUP57-FRB-GFP::His3MX6 NUP170-mCherry::kanMX6*	PCR-based integration using pFA6a-mCherry-kanMX6 and pFA6a-FRB-GFP-His3MX6
PCCPL520	*NUP85-loxP-HA-mCherry-HYG-loxP-GFP CRE-EBD78::HIS3*	PCR-based integration using PLPMR2 and integration of pTW040 linearized with Eco47III
PCCPL522	*NDC1-loxP-HA-mCherry-HYG-loxP-GFP CRE-EBD78::HIS3*	PCR-based integration using PCR-based integration using PLPMR2 and integration of pTW040 linearized with Eco47III
PCCPL523	*kanMX6::pGAL1-3HA-SWE1 NUP85-loxP-HA-mCherry-HYG-loxP-GFP pINT-CRE-EBD78::HIS3*	PCR-based integration using PLPMR2, pFa6a-kanMX6-GAL1-HA integration of pTW040 linearized with Eco47III
PCCPL526	*NSP1-loxP-HA-mCherry-HYG-loxP-GFP pINT-CRE-EBD78::HIS3*	PCR-based integration using PLPMR2 and integration of pTW040 linearized with Eco47III
PCCPL528	HHY110, *NUP192-FRB-GFP::His3MX6 NUP60-mCherry::kanMX6*	PCR-based integration using pFA6a-mCherry-kanMX6 and pFA6a-FRB-GFP-His3MX6

Table S1. **Yeast strains** *(Continued)*

Name	Genotype	Source
PCCPL529	ABY534, *NUP85-GFP::kanMX6*	PCR-based integration using pFA6a-GFP-kanMX6
PCCPL530	W303, *myo4Δ::hphMX6 NUP85-GFP::kanMX6*	Progeny from cross PCCPL65 and BWCPL42
PCCPL532	PCCPL393 *EXO70-mCherry::natMX6*	PCR-based integration using pFA6a-mCherry-natMX6
PCCPL533	PCCPL393, *HDEL-DsRed::TRP1*	Integration of pKW1358 digested with EcoRV in the TRP1 locus
PCCPL534	PCCPL393, *ABP1-mCherry::natMX6*	PCR-based integration using pFA6a-mCherry-natMX6
PCCPL535	PCCPL393, *KAR9-mCherry::natMX6*	PCR-based integration using pFA6a-mCherry-natMX6
PCCPL542	PCCPL393, *MYO2-mCherry::natMX6*	PCR-based integration using pFA6a-mCherry-natMX6
PCCPL543	PCCPL393, *ABP140-mCherry::natMX6*	PCR-based integration using pFA6a-mCherry-natMX6
PCCPL552	PCCPL304, *HMG1-mCherry::kanMX6*	PCR-based integration using pFA6a-mCherry-kanMX6
PCCPL557	W303, *dyn1Δ::hphMX6*	PCR-based integration using pFA6a-hphMX6
PCCPL559	PCCPL557, *NSP1-GFP::His3MX6*	Progeny from cross CPl1234 and PCCPL557
PCCPL561	PCCPL557, *NUP85-GFP::kanMX6*	Progeny from cross BWCPL42 and PCCPL557
WZCPL2	*NUP170-LoxP-HA-mCherry-HYG-LoxP-GFP CRE-EBD78::HIS3*	PCR-based integration using PLPMR2 and integration of pTW040 linearized with Eco47III
WZCPL5	*HHY110 NUP120-FRB-GFP::HIS3 HMG1-mCherry::kanMX6*	PCR-based integration using pFA6a-mCherry-kanMX6 and pFA6a-FRB-GFP-His3MX6

Table S2. **Plasmids**

Name	Description	Reference/source
pFa6a-GFP-kanMX6	Template for PCR-based chromosomal integration of GFP ORF	Longtine et al., 1998
pFa6a-GFP-TRP1	Template for PCR-based chromosomal integration of GFP ORF	Longtine et al., 1998
pFa6a-GFP-HIS3MX6	Template for PCR-based chromosomal integration of GFP ORF	Longtine et al., 1998
pFa6a-kanMX6-GAL1-3HA	Template for PCR-based chromosomal integration of the GAL1-HA ORF	Longtine et al., 1998
pFa6a-mCherry-natMX6	Template for PCR-based chromosomal integration of the mCherry ORF	Longtine et al., 1998
pFa6a-hphMX6	Template for PCR-based chromosomal integration of hphMX6 cassette	Longtine et al., 1998
pFa6a-FRB-GFP-HIS3	Template for PCR-based chromosomal integration of FRB-GFP ORF	Haruki et al., 2008
pFa6a-FRB-HIS3	Template for PCR-based chromosomal integration of the FRB ORF	Haruki et al., 2008
PLPMR2	For chromosomal integration of -loxP-HA-mCherry- hphMX6-loxP-GFP	This study
pTW040	pINT-CRE-EBD78::HIS3, digest with Eco47III to integrate at the *HIS3* locus	Gift from F. van Leeuwen (Verzijlbergen et al., 2010)
pKW2329	pFA6a-Nup133(C)-2xDendra-CaURA3 Integration plasmid for C-terminal tagging of NUP133 with 2x-Dendra; cut HindIII	Gift from K. Weis (Onischenko et al., 2009)
pKW1358	HDEL-DsRED-TRP1 ER marker (integrated in TRP1 locus), digest with EcoRV	Gift from K. Weis (Onischenko et al., 2009)
PLPC19	pRS416-NSP1	This study
PLPC20	pRS416-NIC96	This study

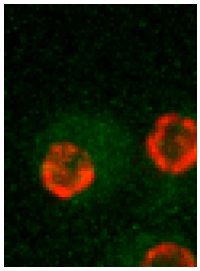

Video 1. **A newly synthesized bud-directed pool of Nsp1.** Cells expressing *NSP1-RITE* incubated in the presence of estradiol and both Nsp1-GFP and Nsp1-mCherry were imaged with a wide-field deconvolution microscope (DeltaVision; Applied Precision/GE Healthcare) every 3 min for 117 min. The video is shown at rate of 3 frames per second (fps).

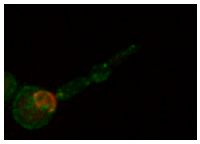

Video 2. **A newly synthesized pool of Nsp1 localizes to the bud in G2-arrested cells.** A *NSP1-RITE* (PCCPL506)–containing strain was grown in the presence of galactose (to induce a G2 arrest) and estradiol (to induce genetic switch to GFP/new form). Nsp1-GFP and Nsp1-mCherry were imaged with a wide-field deconvolution microscope (DeltaVision; Applied Precision/GE Healthcare) every 10 min for 180 min. Video is shown at 3 fps.

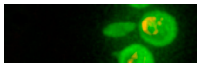

Video 3. **Nup85 distribution in G2-arrested cells.** A *NUP85-RITE* (PCCPL523)–containing strain was grown in the presence of galactose (to induce a G2 arrest) and estradiol (to induce genetic switch to GFP/new form). Nup85-GFP and Nup85-mCherry were imaged with a wide-field deconvolution microscope (DeltaVision; Applied Precision/GE Healthcare) every 10 min for 210 min. The video is shown at 3 fps.

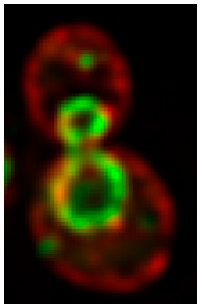

Video 4. **Nsp1-GFP$_{CYT}$ associates with dynamic ER tubules.** *cdc6-1* cells expressing Nsp1-GFP and HDEL-DsRed (PCCPL533) were arrested in G2/M phase for 3 h at 34°C, released for 3 h at RT, and then imaged by a wide-field deconvolution microscope (DeltaVision; Applied Precision/GE Healthcare) at RT every 5 s for 10 min. The video is shown at 10 fps.

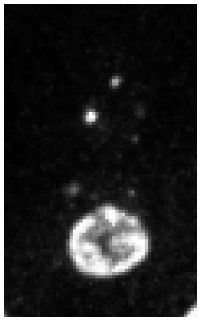

Video 5. **Nsp1$_{CYT}$ foci are connected to the mother NE.** *cdc6-1* cells expressing Nsp1-GFP (PCCPL393) were arrested in G2/M phase for 3 h at 34°C and then imaged with a wide-field deconvolution microscope (DeltaVision; Applied Precision/GE Healthcare) at RT every 3 min for 180 min. The video is shown at 5 fps.

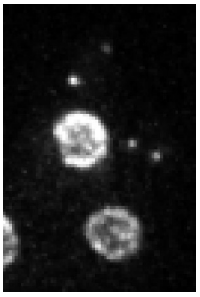

Video 6. **Nsp1$_{CYT}$ foci are connected to the mother NE.** *cdc6-1* cells expressing Nsp1-GFP (PCCPL393) were arrested in G2/M phase for 3 h at 34°C and then imaged with a wide-field deconvolution microscope (DeltaVision; Applied Precision/GE Healthcare) at RT every 3 min for 180 min. The video is shown at 5 fps.

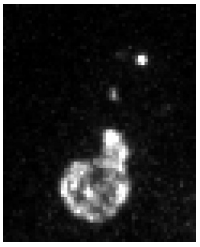

Video 7. **Nsp1$_{CYT}$ foci are connected to the mother NE.** *cdc6-1* cells expressing Nsp1-GFP (PCCPL393) were arrested in G2/M phase for 3 h at 34°C and then imaged with a wide-field deconvolution microscope (Deltavision; Applied Precision/GE Healthcare) at RT every 3 min for 180 min. The video is shown at 5 fps.

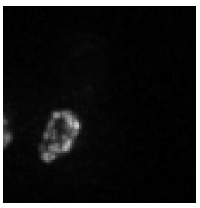

Video 8. **Nup170-GFP distribution during NP formation.** *cdc6-1* cells expressing Nup170-GFP (PCCPL392) were arrested in G2/M phase for 3 h at 34°C and then imaged with a wide-field deconvolution microscope (DeltaVision; Applied Precision/GE Healthcare) at RT every 3 min for 180 min. The video is shown at 3 fps.

References

Haruki, H., J. Nishikawa, and U.K. Laemmli. 2008. The anchor-away technique: rapid, conditional establishment of yeast mutant phenotypes. *Mol. Cell.* 31:925–932. http://dx.doi.org/10.1016/j.molcel.2008.07.020

Keaton, M.A., E.S.G. Bardes, A.R. Marquitz, C.D. Freel, T.R. Zyla, J. Rudolph, and D.J. Lew. 2007. Differential susceptibility of yeast S and M phase CDK complexes to inhibitory tyrosine phosphorylation. *Curr. Biol.* 17:1181–1189. http://dx.doi.org/10.1016/j.cub.2007.05.075

Liang, C., M. Weinreich, and B. Stillman. 1995. ORC and Cdc6p interact and determine the frequency of initiation of DNA replication in the genome. *Cell.* 81:667–676. http://dx.doi.org/10.1016/0092-8674(95)90528-6

Longtine, M.S., A. McKenzie III, D.J. Demarini, N.G. Shah, A. Wach, A. Brachat, P. Philippsen, and J.R. Pringle. 1998. Additional modules for versatile and economical PCR-based gene deletion and modification in *Saccharomyces cerevisiae*. *Yeast.* 14:953–961. http://dx.doi.org/10.1002/(SICI)1097-0061(199807)14:10<953::AID-YEA293>3.0.CO;2-U

Onischenko, E., L.H. Stanton, A.S. Madrid, T. Kieselbach, and K. Weis. 2009. Role of the Ndc1 interaction network in yeast nuclear pore complex assembly and maintenance. *J. Cell Biol.* 185:475–491. http://dx.doi.org/10.1083/jcb.200810030

Schott, D., J. Ho, D. Pruyne, and A. Bretscher. 1999. The COOH-terminal domain of Myo2p, a yeast myosin V, has a direct role in secretory vesicle targeting. *J. Cell Biol.* 147:791–808. http://dx.doi.org/10.1083/jcb.147.4.791

Verzijlbergen, K.F., V. Menendez-Benito, T. van Welsem, S.J. van Deventer, D.L. Lindstrom, H. Ovaa, J. Neefjes, D.E. Gottschling, and F. van Leeuwen. 2010. Recombination-induced tag exchange to track old and new proteins. *Proc. Natl. Acad. Sci. USA.* 107:64–68. http://dx.doi.org/10.1073/pnas.0911164107